J Radiol Clin Imaging 2021; 4 (4): 141-158 *DOI: 10.26502/jrci.2809051s*

Review Article

Thoracic Boundary Pathology: Radiological Investigation and Review

Maria Chiara Imperato*, Riccardo Monti, Salvatore Cappabianca, Ferdinando Caranci, Renata Conforti

Department of Precision Medicine, Università degli Studi della Campania "Luigi Vanvitelli", Naples, Italy

***Corresponding Author:** Maria Chiara Imperato MD, Department of Precision Medicine, Università degli Studi della Campania "Luigi Vanvitelli", 80138 Naples, Italy

Received: 14 October 2021; **Accepted:** 01 November 2021; **Published:** 15 November 2021

Citation: Maria Chiara Imperato, Riccardo Monti, Salvatore Cappabianca, Ferdinando Caranci, Renata Conforti. Thoracic Boundary Pathology: Radiological Investigation and Review. Journal of Radiology and Clinical Imaging 4 (2021): 141-158.

Abstract

Thoracic paravertebral masses are a diagnostic challenge due to the broad spectrum of lesions that may be found in this compartment. The correct radiological approach is essential to narrow the differential diagnoses but, due to the overlap of imaging features of certain lesions, in selected cases, a pathological study may be necessary.

Keywords: Thoracic paravertebral compartment; Paravertebral lesions; Neurogenic tumors; FNAC

Abbreviations: CT- Computed tomography; MRI- Magnetic resonance imaging; FNAC- fine-needle aspiration cytology; PNST- Peripheral nerve sheath tumor; MPNST- Malignant peripheral nerve sheath tumor; NF1 - Neurofibromatosis type 1; NF2- Neurofibromatosis type 2; ADC- Apparent diffusion coefficient

1. Introduction

The paravertebral compartment can present various lesions whose spectrum ranges from inflammatory to malignant ones. The presence of a paravertebral mass, whether symptomatic or not, entails a diagnostic challenge and always causes concern. Patients can be asymptomatic or complain about radicular or back pain and neurological deficits related to spinal cord compression. Computed tomography (CT) and magnetic resonance imaging (MRI) play an important role in the mass characterization and the assessment of adjacent structures invasion. Although CT is more accurate compared to MRI in the evaluation of bone involvement, MRI offers a better and useful soft-tissue contrast of lesions. On the other hand, although MRI has well-established criteria to distinguish inflammatory from malignant disease, these are, at times, fallible. Therefore, despite the formidable armamentarium of diagnostic tools now available, it is still difficult, in many cases, to give more than a narrowed differential diagnosis.

Since optimal therapy depends upon the cyto/histopathology of the lesion, the percutaneous fine-needle aspiration cytology (FNAC) has been established as a useful diagnostic technique that can facilitate patient management and preoperative decision making, avoiding unnecessary and invasive surgical procedures. Obtaining cytologic material in infectious/inflammatory lesions allows both rapid identification of the pathogenic microorganism and initiation of treatment in many cases. CT provides an accurate localization and delineation of the lesion including both the osseous and the extra-osseous components, a safe access route to the lesion, and also documents accurate needle placement within the lesion.

In our retrospective observational study, we report our experience with paravertebral lesions considering in particular bone involvement and differential diagnosis.

2. Discussion

Thoracic paravertebral compartment includes thoracic vertebrae, spinal cord and paravertebral soft tissues; it is defined by the following boundaries: superiorly the thoracic inlet, inferiorly the diaphragm, the visceral compartment in front, and posterolaterally a vertical line along the posterior margin of the chest wall at the lateral aspect of the transverse processes [1, 2].

Thoracic paravertebral masses are boundary lesions between visceral and neurogenic compartments, including a heterogeneous group of lesions, then may have several different histopathologic origins. Neurogenic tumors are the most common encountered masses and consist of peripheral nerve sheath tumors (schwannoma, neurofibroma, malignant peripheral nerve sheath tumor); parasympathetic ganglia tumors (paraganglioma, chemodectoma, pheochromocytoma); sympathetic chain tumors (neuroblastoma, ganglioneuroblastoma, ganglioneuroma).

In the thoracic paravertebral region, even non-neurogenic tumors may be found and include chordoma, chondrosarcoma, Ewing's sarcoma, esophageal neoplasm, lymphoma, invasive thymoma and metastasis. Other potential pathologies of this compartment are infections (discitis, osteomyelitis, paravertebral abscesses), inflammation (mediastinitis, sarcoidosis, lymphoid hyperplasia, pancreatic pseudocyst); traumatic lesions (paraspinal hematoma), lymphadenopathy, extramedullary hematopoiesis, foregut duplication cysts, neurenteric cyst,

esophageal duplication cyst, bronchogenic cyst and thoracic meningocele, hernias (hiatus hernia, Bochdalek hernia) and vascular lesions (thoracic aortic aneurysm, varices, lymphangioma).

Nonspecific pain and neurological deficits appear during the progression of the process and may cause irreversible sequela. In patients presenting with pain and/or neurologic dysfunction, a detailed medical examination is indispensable, but also imaging studies should be performed. The differential diagnosis between thoracic paravertebral masses is not always simple because there may be overlap in the imaging appearances, but clinical information combined with some specific imaging features and in particular patterns of bone involvement (bone infiltration and extension to spinal canal through intervertebral foramina), can close the diagnosis. The correct radiological approach to these lesions represents a fundamental element in the diagnostic process, the first things to evaluate are the location of the lesion and the identification of the most probable structure of origin, followed by its extension (if the lesion is bilateral and/or multifocal) and its growth pattern, vertebral and discal involvement, tissue characteristics and pattern of enhancement after intravenous contrast injection.

3. Neurogenic Tumors

3.1 Peripheral nerve sheath tumors

Peripheral nerve sheath tumors (PNSTs), arise from spinal nerve roots and are divided into benign (schwannoma and neurofibroma) and malignant (malignant peripheral nerve sheath tumor) lesions. Schwannomas and neurofibromas are the most common benign intradural-extramedullary spinal tumors, they usually are solitary, but they can be multiple in patients with neurofibromatosis type 2 (NF2) and neurofibromatosis type 1 (NF1) respectively [2, 3]. Both may cause widening of the intervertebral foramina with extraspinal extension showing a typical appearance called the “dumbbell shape” sign [4]. Bone pressure erosion of adjacent vertebral bodies and ribs and calcifications are seen more frequently in neurofibromas than in schwannomas, while schwannomas can show hemorrhage, cystic areas, and/or adipose degeneration, which are usually absent in neurofibromas [5].

On CT schwannomas appear as hypodense lesions with spherical or elliptical morphology and well-defined margins; contrast-enhanced CT may show homogeneous enhancement when the mass is small or heterogeneous enhancement in larger schwannomas due to cystic and hemorrhagic components [5]. Generally, on MRI studies, schwannomas show low to intermediate signal intensity on T1w images and hyperintense or heterogeneous signal in T2w images with focal areas of hyperintensity, which indicate cystic or myxoid degeneration within the tumor (Figure 1). They are characterized by intense contrast enhancement [6]. Totally cystic schwannomas are rare and appear hypointense on T1w and hyperintense on T2w images [7]. Cystic schwannoma has to be differentiated from Tarlov cyst, arachnoid cyst, neurenteric cyst, epidermoid cyst, and cystic teratoma but compared to these cystic lesions it has a well-enhancing wall.

Spinal neurofibromas originate from the nerve sheath and typically encase the nerve roots due to an asymmetric growth pattern [8]. On CT studies neurofibromas demonstrate soft-tissue attenuation, but areas of hyperdensity may be present; they may show confluent or, more typically, peripheral areas of contrast enhancement due to the presence of cellular and

fibrous elements, whereas central myxomatous and cystic regions are hypovascular [3]. On MRI studies neurofibromas show low to intermediate signal intensity on T1w sequence and heterogeneous enhancement after intravenous gadolinium administration. On T2w sequence they appear heterogeneous: T2 high signal intensity regions correspond to areas of myxoid tissue or cystic degeneration, while areas of low signal intensity correspond to collagen and fibrous tissue (Figure 2).

Paravertebral neurofibromas may extend into the spinal canal and mimic extramedullary hematopoiesis, other neurogenic tumors or neurenteric cysts [3]. Plexiform neurofibromas represent a neurofibroma variant in up to 50 % of patients with NF1 and appear as segments of diffusely and irregularly enlarged nerves and nerve branches, resulting in not circumscribed and locally invasive lesions with typical "bag of worms" appearance on MRI [9]. On CT plexiform neurofibromas appear as a hypodense lesion and on MRI examination they are hypointense on T1w and hyperintense on T2w sequences with moderate gadolinium enhancement; on T2w images they may show the “target sign” due to a central area of hypointensity with a peripheral hyperintensity [10]. Plexiform neurofibromas located in the paraspinal area, can grow and extend laterally along the spinal nerves with or without the involvement of the neural foramina [11].

In NF1 there may be other spinal manifestations such as acute kyphoscoliosis at the cervical-thoracic junction and vertebral body anomalies (vertebral scalloping, neural foramina widening and transverse process spindling), and soft-tissue abnormalities such as dural ectasia [12]. The differential diagnosis includes meningocele, which is usually cystic and can also occur in patients with NF1[13].

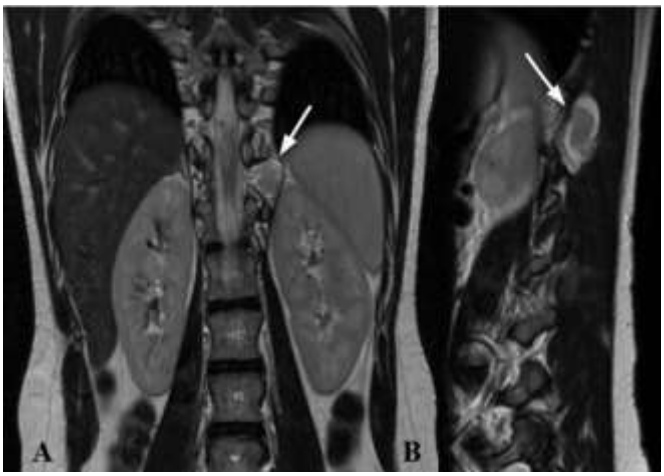

Figure 1: MRI of a 16 years old patient with NF2. Coronal T2w (A) and sagittal T2w (B) show at D11 level on the left posterior paramedian and median region a well-defined lesion (white arrow) with heterogeneous signal on T2w images with peripheral areas of hyperintensity, which indicates cystic or myxoid degeneration.

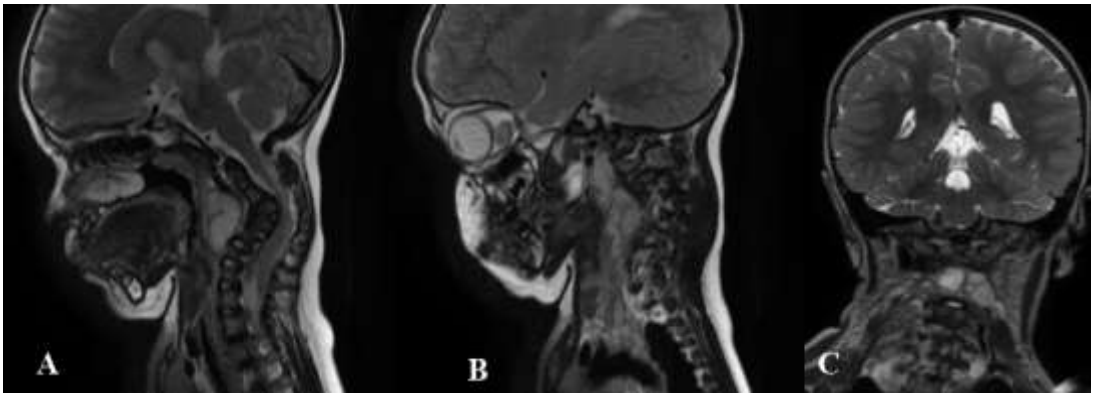

Figure 2: Boundary lesion between cervical and thoracic vertebrae in a 2 years old patient with NF1. MRI sagittal T2w - paramedian right (A) and left (B) - and coronal T2w (C). Pathologic tissue in prevertebral and paravertebral spaces, extending from C2 to D3, with plexiform features on the right side, where it involves deep and superficial muscular structures. This lesion extends in the right neural foramina between C3-C4 and C4- C5, and posteriorly in the epidural tract between C3, C4 and C5.

Malignant peripheral nerve sheath tumors (MPNSTs) are soft tissue malignant tumors that typically arise from simple or plexiform neurofibromas, and rarely from the malignant transformation of schwannomas. They show rapid growth, irregular borders and variable differentiation [14]. On CT, they appear as hypodense masses with moderate enhancement, areas of lower attenuation correspond to central hemorrhage and necrosis; calcifications may be present. These lesions may be responsible for adjacent bone erosion and compression or invasion of mediastinal structures and adjacent chest wall.

On MRI, MPNSTs are typically isointense on T1w and hyperintense on T2w imaging with preferential peripheral enhancement, although the MRI appearance can vary depending on size and internal cystic, hemorrhagic, or necrotic changes [15]. The main differential diagnosis is with benign nerve sheath tumors but some imaging features can help: rapid dimension increase of the mass, peripheral enhanced pattern, perilesional edema-like zone and intratumoral cystic areas [16].

3.2 Autonomic nervous system tumors

Autonomic nervous system tumors include a spectrum of lesions ranging from purely benign encapsulated ganglioneuromas to malignant ganglioneuroblastomas to aggressively malignant neuroblastomas. Nonaggressive autonomic nervous lesions generally manifest as well-defined, oblong masses growing parallel to the spine, typically spanning three to five vertebrae [17]. A way to differentiate these tumors from peripheral nerve sheath tumors is the morphology: PNSTs tend to be spherical while the autonomic neurogenic lesions are more cylindrical and extend in a longitudinal direction; moreover, calcifications are more common in autonomic nervous tumors when compared with nerve sheath tumors [17].

Ganglioneuromas are well-differentiated neuronal tumors, usually attached to either a sympathetic nerve or to an intercostal nerve trunk, that tend to be slow-growing and thus less aggressive on adjacent structures compared with neuroblastomas [17]. On unenhanced CT, they may show low internal attenuation corresponding to abundant myxoid matrix. Approximately 20% of ganglioneuromas may show calcifications with a typical fine and speckled pattern [17]. Slight to moderate enhancement can be seen on contrast-enhanced CT [18]. MRI characteristics of ganglioneuromas include homogeneous, intermediate signal intensity on all sequences with an occasional whorled appearance of low-signal-intensity curvilinear or nodular bands on T1w and T2w images [17]. Paravertebral ganglioneuromas can extend through the neural foramina involving the spinal canal epidural space.

The differential diagnosis with spinal neuroblastoma and ganglioneuroblastoma is not easy considering only imaging features, but the presence of metastases is suggestive for neuroblastoma or ganglioneuroblastoma, while the presence of calcifications is more common in neuroblastomas. Ganglioneuroblastoma is a transitional tumor containing elements of both malignant neuroblastoma and benign ganglioneuroma. They may be encapsulated and are commonly attached to the nerve trunk. CT findings are variable from a homogeneous solid mass to a predominantly cystic mass with a few thin strands of soft-tissue attenuation [18].

On MRI they appear hypointense on T1w images, heterogeneously hyperintense on T2w images, and intensely enhanced after intravenous administration of gadolinium. However, Gahr et al. [19] found a significant difference in the apparent diffusion coefficient (ADC) of neuroblastoma compared with the ADC of ganglioneuroma or ganglioneuroblastoma, suggesting that the evaluation of ADC maps values could differentiate neuroblastoma from ganglioneuroma or ganglioneuroblastoma. Neuroblastomas have no capsule and frequently contain extensive areas of hemorrhage, necrosis, and cystic degeneration. They may be locally invasive and widely metastatic [17].

The appearance on CT can range from a homogeneous solid to a predominantly cystic or hemorrhagic mass, that shows either heterogeneous or mild enhancement [20, 21]. Thoracic neuroblastomas often show coarse, finely stippled, or curvilinear calcifications on CT [21]. MRI shows homogeneous or heterogeneous signal intensity on all sequences. MR images after intravenous administration of gadolinium can show both homogeneous to heterogeneous enhancement, with a more heterogeneous appearance in larger tumors. High signal intensity may be seen from hemorrhage on T1w images and cystic change on T2 w images [17].

The main differential diagnoses for thoracic neuroblastoma are lymphoma, extralobar pulmonary sequestration, ganglioneuroma and ganglioneuroblastoma.

3.3. Paraganglioma

Paragangliomas arise from neuroectodermally derived chemoreceptor paraganglionic cells of the sympathetic or parasympathetic chains. Thoracic paragangliomas rate of malignancy is greater than primary paragangliomas in other locations [18]. On CT they appear as homogeneous masses with intense enhancement due to their rich vascularization, sometimes calcifications are present. Areas of osteolysis or

even pathological fractures and/or enlargement of the vertebral foramina are often observed [22] Some tumors may show hemorrhage or cystic degeneration, which results in areas of low attenuation on CT. On MRI, paragangliomas appear hypo-isointense on T1w images and slightly hyperintense on T2w images, when large enough, the mass may have a salt-and-pepper appearance from vessel signal flow voids scattered with hyperintense foci; they show an intense homogeneous enhancement after gadolinium administration [23].

The diagnosis of paraganglioma cannot be based only on imaging features, definitive diagnosis is possible after the histological exam; the differential diagnosis of paragangliomas includes schwannomas, ganglioneuromas, secondary lesions and some posterior mediastinal tumors. They may be distinguished from more malignant lesions when compression and dislocation are present instead of infiltration. Compared to myelomas or metastasis, paraganglioma vascularization is not only rich but also homogeneous [24].

4. Non-Neurogenic Tumors

4.1 Lymphoma

Spinal lymphoma is an extranodal lymphoma and a relatively uncommon spinal tumor, it usually arises in the epidural or intramedullary spaces. The diagnosis of primary epidural spinal lymphoma entails the exclusion of any other identifiable location of lymphoma [25]. These primary tumors are most commonly located in the thoracic spine, followed by the cervical spine and less commonly in the lumbar spine [26]. Spinal lymphoma seems to arise from the paraspinal soft tissues such as the paravertebral ganglions or the epidural lymphoid tissues and then it can extend through the intervertebral foramen without causing bone erosion [27]. Bone sparing is a characteristic of spinal lymphomas, in contrast to other tumors where vertebral bone destruction and spinal cord invasion are often detected [28].

CT suggests the diagnosis of spinal lymphoma when a soft tissue density mass without bone destruction or erosion is observed (Figure 3), although rarely, it has been found. On MRI (Figure 3) spinal lymphoma appears as iso- or hypointense homogeneous tumor with marked contrast enhancement and possible foraminal extension [25]. Moreover, even if the pathologic tissue does not usually show bony erosion of contiguous vertebral bodies, it is associated with signal alteration of multiple vertebral bodies in relation to bone marrow replacement phenomena. The diagnosis of spinal lymphoma requires a CT-guided biopsy when bone marrow biopsy and blood tests results are inconclusive; the differential diagnosis includes metastasis, meningioma, neurofibroma, malignant peripheral nerve sheath tumors and leukemic masses.

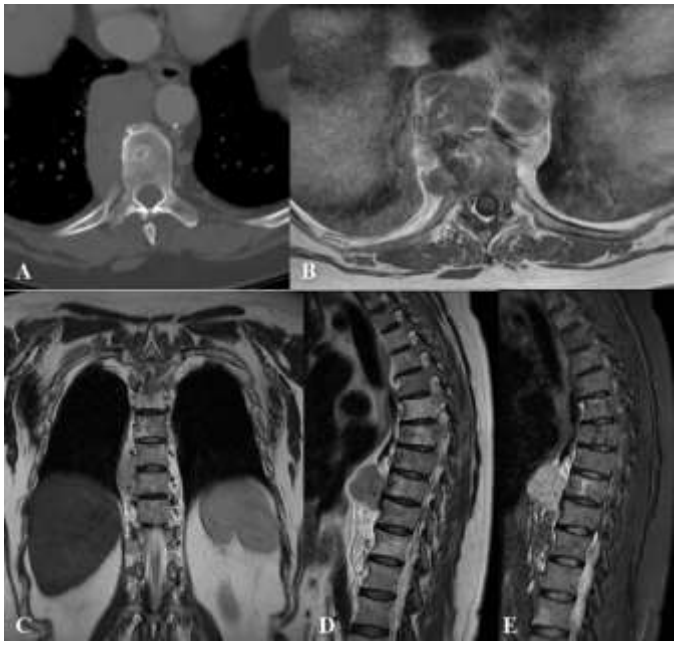

Figure 3: Non-Hodgkin lymphoma paravertebral lesion in a 68 years old female patient. Axial CT scan (A), hypodense expansive mass with significant contrast enhancement in the right paravertebral space, no bone erosion is found. MRI - axial T1w after contrast injection (B), coronal T2w (C), sagittal T2w (D) and STIR (E) – of the polylobular lesion in the paravertebral and right retrocrural space of D8-D10 tract, low signal at T1w images with homogeneous enhancement after intravenous gadolinium administration, this mass occupies the costovertebral space but does not show signs of erosion of the contiguous vertebral bodies.

4.2 Ewing's sarcoma

Ewing's sarcoma is one of the most common malignant bone tumors occurring in children and young adults, it can affect any bone but the most common sites are the lower extremities, followed by the pelvis, upper extremities, axial skeleton, and ribs and face [29]. CT scans of Ewing's sarcoma typically show a large ill-defined mass with an inhomogeneous appearance determined by solid components and cystic degeneration, which may be accompanied by calcifications. The expansion of an Ewing's sarcoma of the chest wall may cause lung collapse or infiltration [30]. On MR T1w images these tumors are generally iso- hyperintense and larger tumors appear as heterogeneous masses whereas smaller ones tend to be more homogeneous; on T2w images they tend to have heterogeneous high signal intensity (Figure 4).

Moreover, Ewing's sarcomas show marked enhancement after intravenous administration of gadolinium. When tumors arise in the paravertebral region can determine extrinsic bone erosion; secondary bone reaction in the adjacent vertebral body and direct extension through the neural foramen may also be seen [30, 31].

Imaging techniques are mainly used to evaluate the tumor extension and a definitive diagnosis is obtained only after biopsies or surgical removal. Ewing's sarcoma periosteal reaction may be difficult to differentiate from other bone tumors and osteomyelitis, which is the most common differential diagnosis. The differential diagnosis also includes other malignant tumors such as chondrosarcoma, fibrosarcoma, and soft-tissue sarcomas, although these usually occur in patients older than those with Ewing's sarcoma [32].

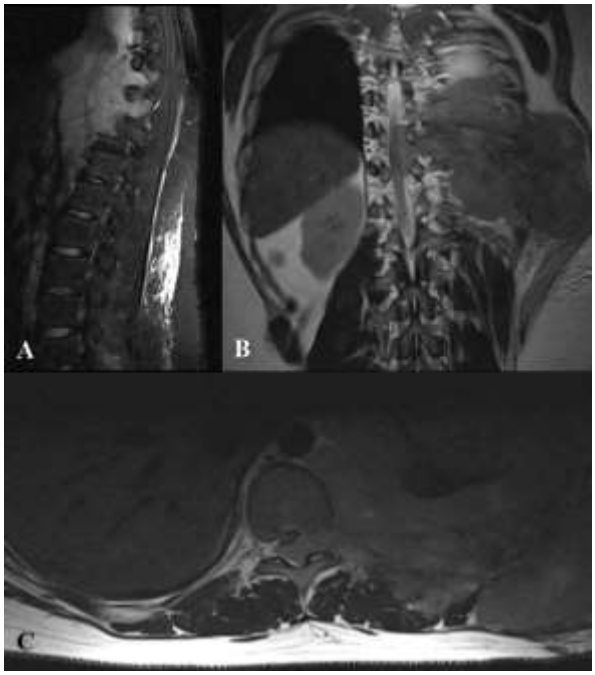

Figure 4: Paravertebral extension of Ewing's sarcoma in a 17 years old male patient. MRI - sagittal T2w tirm (A), coronal T2w (B), axial T2w (C) large heterogeneous left chest wall mass associated with ribs destruction and incipient thoracic vertebral bodies involvement and extension to the spinal canal, the lesion is hypointense on T1w and hyperintense on T2w images. The left lung was compressed due to the mass effect.

4.3 Synovial sarcoma

Synovial sarcoma is a rare soft-tissue malignant neoplasm, most often diagnosed in adolescents or young adults, it usually arises near a large joint in the extremities (especially the knee), and paravertebral location is extremely rare [33]. On CT synovial sarcoma appears heterogeneous with a density similar to or slightly lower than muscles (Figure 5). Areas of lower attenuation represent necrosis or previous hemorrhage, although smaller lesions tend to be more homogeneous. CT scans obtained after intravenous contrast administration show heterogeneous enhancement; on CT cortical bone erosion and periosteal reaction have been reported.

On T1w MR images, synovial sarcoma usually appears iso or slightly hyperintense, on T2w images it is heterogeneously hyperintense with an appearance that results in the so-called "triple sign", due to high signal areas of necrosis and cystic degeneration, relatively high signal soft tissue components and areas of low signal intensity due to dystrophic calcifications, and fibrotic bands; after gadolinium intravenous administration it shows heterogeneous enhancement [32] (Figure 5).

The most common differential diagnosis includes chondrosarcoma, extraskeletal Ewing's sarcoma, lymphoma and benign neurogenic tumors. Benign tumors generally show smooth margins and lack of infiltrative growth, but even paravertebral malignant tumors with epidural extension may show similar imaging findings so the final diagnosis depends on the histologic findings [34].

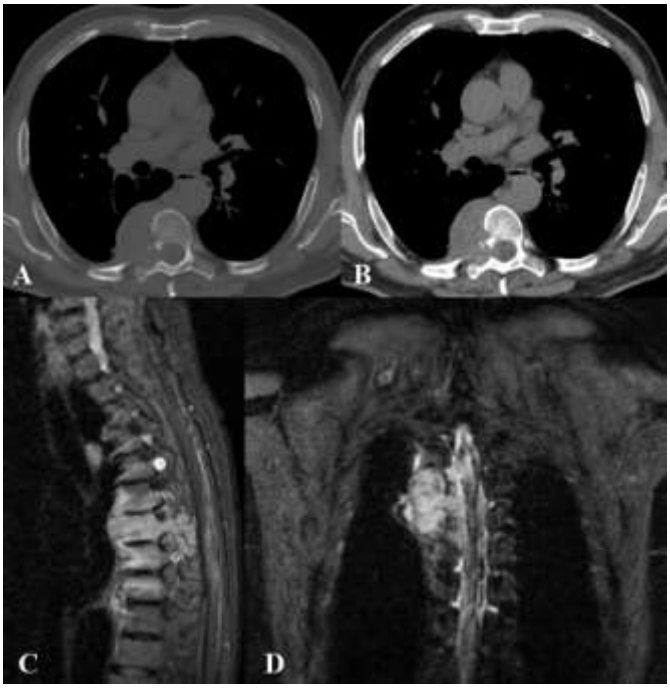

Figure 5: Spindle cell sarcoma in a 64 years old male patient. Axial CT images (A, B) show inhomogeneous soft tissue density, resulting in erosion of the cortical of the right D7 hemisoma, right D7 lamina, head and neck of the right 7th rib. Invasion and enlargement of the correspondent neural foramen with compression of the spinal cord. MRI (C, D) shows a coarse heteroplastic mass in the right posterior paravertebral region, at the level of the costovertebral angle, between D6-D8, showing hypointense T1 signal and inhomogeneous enhancement after intravenous administration of gadolinium. This lesion infiltrates the right hemiportion of the posterior arch and soma of D7, extends to intervertebral foramina and shows the absence of cleavage plane with ipsilateral pleura.

4.4 Spine metastases

The spine is the most common site of bone metastases, which derive mainly from breast, lung, prostate, and kidney cancer [35]. Spine metastases can determine bone destruction and vertebral collapse, invasion of paravertebral tissues, nerve roots or spinal cord compression, enlargement of the neural foramina, and scalloping of the posterior borders of the vertebral body. Focal bony lesions appear hypointense on T1w and hyperintense on T2w images, while sclerotic lesions appear hypointense on all sequences. Diffuse abnormal bone marrow signal may be observed. Post-contrast T1w images delineate the enhancing metastases as well as associated paraspinal and epidural lesion extension. Epidural soft tissue is commonly associated with the destruction of vertebrae and direct extension through the posterior longitudinal ligament, or extension through the intervertebral foramina [36] (Figure 6). A biopsy is advisable in all patients without a diagnosis of a primary tumor. It can be performed via percutaneous needle biopsy guided by CT or an open biopsy [37].

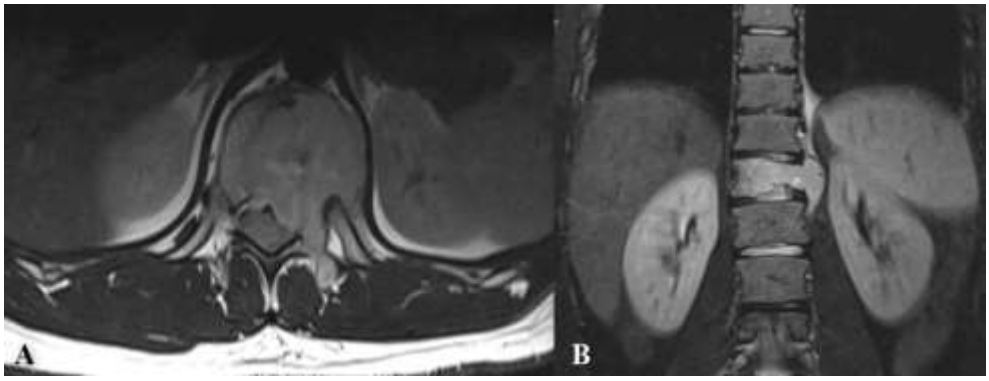

Figure 6: Sarcoma vertebral metastases in a 23 years old male patient MRI - axial T1w (A) and coronal T2w (B) - reveals the vertebral lesion of D11 with high signal intensity on T2w images extending to the left paravertebral space.

5. Non-Neoplastic Lesions

5.1 Extramedullary hematopoiesis

Extramedullary hematopoiesis refers to the ectopic development of hematopoietic tissue outside the bone marrow. It usually presents in patients suffering from hematologic diseases resulting in hemolytic anemia (thalassemia, sickle cell anemia, hereditary spherocytosis) and bone marrow replacement (myelofibrosis, chronic myelogenous leukemia). In the paraspinal thoracic regions, extramedullary hematopoiesis usually originates from the costovertebral angles; it can be unilateral or bilateral, as multiple contiguous foci like a tumor-like lesion, which makes differential diagnosis difficult. The mass usually does not determine bony destruction, but the epidural extension of extramedullary hematopoiesis tissue may cause spinal cord compression (Figure 7) [38]. CT and MRI allow the evaluation of the lesion in various stages of the disease evolution. The paraspinal active hematopoietic masses are well marginated; on CT they show soft-tissue-like density and on MRI reveal intermediate signal intensity in both T1w

and T2w images, with mild homogeneous enhancement after intravenous contrast administration [39].

In patients treated with blood transfusions, the extramedullary paraspinal foci of hematopoiesis may decrease in size and show massive iron deposition: in this case, the lesion shows high CT density and low intensity in both T1w and T2w images without enhancement after contrast intravenous administration [40]. In non-transfused and non-chelated patients can be observed foci with fatty content. Fatty degeneration is most probably related to oxidative stress leading to lipid peroxidation of cell membranes and production of oxygen free radicals [40].
Finally, older inactive lesions show both increased CT density due to iron deposit or low density due to fatty infiltration and also high signal intensity in both T1w and T2w MRI sequences as a consequence of fatty infiltration or low signal intensity in both T1w and T2w MRI sequences due to iron deposition [40]. Differential diagnosis is often easy, based on the patient clinical presentation and in case of multifocal lesions, characteristic localization, and iron deposition or fatty replacement, but when a solitary, unilateral active lesion, is found, other lesions including metastatic malignant disease, lymphoma, multiple myeloma, vascular anomalies and epidural abscesses [41], should be excluded. Biopsy should be reserved for older patients with a high probability of malignant disease and if the clinical and radiological picture is equivocal [38].

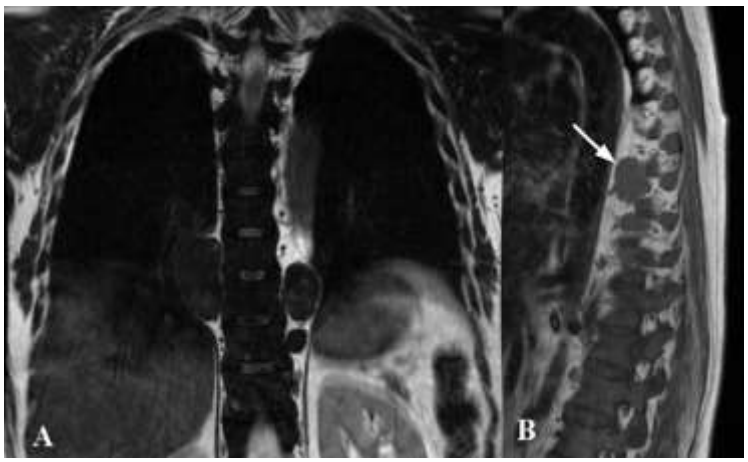

Figure 7: Paravertebral foci of extramedullary hematopoiesis in a 48 female patient suffering from thalassemia. MRI - coronal T2w (A) and sagittal T1w (B) images - shows oval homogeneous and well-marginated lesions corresponding to ectopic hematopoietic tissue in the right paravertebral side at D8-D9 level, and in the left paravertebral side on D9 level (white arrow in B).

5.2 Infectious diseases

Spinal infections are typically caused by bacteria or mycobacteria and usually start in the anterior portion of the vertebral body, because of its rich arterial supply, and then involve the rest of the vertebra. The most common infecting organism is *Staphylococcus aureus*, which is seen in 55%–90% of cases. Pyogenic spondylitis usually involves two contiguous vertebral bodies and the intervening disc determining vertebral endplates and disc destruction with loss of vertebral height [42-44]. CT findings include ill-defined soft tissue, unorganized fluid or loculated collection in the paravertebral compartment, infiltration of paraspinal fat and hyperdensity of intervertebral disc; in the final phases may be present osseous erosion, disc space narrowing and sequestrum development. On MRI involved vertebral bodies show hypointensity on T1w sequences, with loss of definition of the vertebral endplate, and hyperintensity on T2w images due to bone marrow edema; the involved disc space shows fluid-like signal intensity on both T1w and T2w images [44, 45] (Figure 8). After intravenous administration of gadolinium, different disc enhancement patterns can be found: homogeneous enhancement of most of the disc, patchy non-confluent areas of enhancement and thick or thin areas of peripheral enhancement [46].

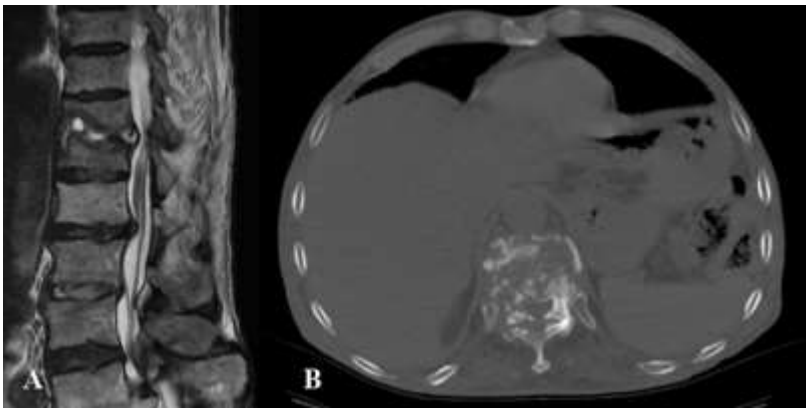

Figure 8: Pyogenic discitis and osteomyelitis of D11- D12 in a 67 years old male patient with back pain. A) Sagittal T2w MRI image shows D 11 - D 12 disco-vertebral complex morphological and signal changes consisting of erosion of vertebral endplates and fluid within the disc. The morpho-structural alterations determine the compression of the adjacent anterior epidural space and the anterior portion of the medullary cone, with myelopathy signs at the same level; B) Axial CT image shows D11-D12 diffuse vertebral soma and peduncles destruction, evidence of diffuse abscesses that extend bilaterally in the paravertebral spaces.

The differential diagnosis with tuberculosis is not always easy, but Tuberculosis can involve even the posterior vertebral portions, rarely involves the neighboring disks, and compared to pyogenic spondylitis the Tuberculosis infection typically shows more sharply destructive margins with the absence of reactive sclerosis. If not treated the infection spreads to the prevertebral and paravertebral spaces, between 55 and 96 % of paraspinal abscesses occur in the thoracic

spine [47]. CT may show vertebral body destruction and sometimes bony fragments migrate into adjacent soft tissue. After administration of intravenous contrast, it is possible to observe multiloculated cystic paraspinal masses, enhancing granulomatous tissue and the walls of abscesses located in both bone and soft tissues [47]. On MRI the signal intensity of vertebral bodies decreases on T1w sequences, while signal increases in both T2w and STIR (short tau inversion recovery) sequences, as a result of the replacement of bone marrow by inflammatory exudates, cells and hyperemia. Abscesses often show high signal intensity on T1w images with reduced signal intensity on T2w sequences, compared to the cerebrospinal fluid signal. After intravenous administration of gadolinium, the abscess shows a thin and smooth wall enhancement [47] (Figure 9).

Figure 9: Tuberculosis spondylitis in an 18 years old patient. MRI - coronal T2w (A), sagittal T2w (B), axial T2w (C), axial T1w after gadolinium injection (D). Height and morphology alterations of the D10 and D9 vertebrae, with somatic collapse associated with pathological modification of the spongiosa signal and with initial extension to the interposed intersomatic disc. Inflammatory material wraps around D8, D9 and D10 vertebral bodies extending through the correspondent intervertebral foramina. The process also extends to the anterior epidural space between D8 and D10 where it compresses and dislocates posterolaterally the spinal cord. After intravenous gadolinium administration, intense and inhomogeneous vertebral enhancement and necrotic colliquative perivertebral material are visible.

Degenerative and inflammatory spinal diseases may mimic spinal infection; in most cases, MRI patterns ease the differentiation of infectious spondylitis from other conditions such as discogenic vertebral body degeneration in the inflammatory phase, ankylosing spondylitis and SAPHO (Synovitis, Acne, Pustulosis, Hyperostosis and Osteitis) syndrome [48]. Atypical forms of spinal tuberculosis can be indistinguishable from paravertebral neurofibromas, lateral meningoceles and lymphoma [49]. When blood cultures are negative or when a polymicrobial infection is suspected percutaneous CT-guided biopsy is necessary to identify the spondylodiscitis origin [50].

6. Conclusions

The diagnosis in thoracic boundary lesions might be difficult to determine due to the broad variety of lesions that can affect this district and the overlapping of imaging appearances, but the correct radiologic approach associated with clinical information may help to narrow the differential diagnosis. Imaging modalities have complementary roles in the evaluation of paravertebral lesions, CT best evaluates osseous involvement while MRI is better for the assessment of soft tissue involvement, but when the information provided by these techniques is not sufficient, direct assessment through biopsy is necessary.

Conflicts of Interest

The authors certify that there is no conflict of interest with any financial organization regarding the material discussed in the manuscript.

References

1. Carter BW, Benveniste MF, Madan R, et al. ITMIG Classification of Mediastinal Compartments and Multidisciplinary Approach to Mediastinal Masses. Radiographics 37 (2017): 413-436.
2. Pavlus JD, Carter BW, Tolley MD, et al. Imaging of Thoracic Neurogenic Tumors. AJR 207 (2016): 552-561.
3. Fortman BJ, Kuszyk BS, Urban BA, et al. Neurofibromatosis type 1: a diagnostic mimicker at CT. Radiographics 21 (2001): 601-612.
4. Nakazono T, White CS, Yamasaki F, et al. MRI Findings of Mediastinal Neurogenic Tumors AJR 197 (2011): W643-W652.
5. Mussetto I, Matos J, Romano N, et al. A giant spinal schwannoma mimicking a renal mass: A case report. Radiology Case Reports 13 (2018): 805-809.
6. Crist J, Hodge JR, Frick M, et al. Magnetic Resonance Imaging Appearance of Schwannomas from Head to Toe: A Pictorial Review J Clin Imaging Science 7 (2017): 38.
7. Kumar S, Gupta R, Handa A, et al. Totally cystic intradural schwannoma in thoracic region Asian Journal of Neurosurgery 12 (2017).
8. Abul-Kasim K, Thurnher MM, McKeever P, et al. Intradural spinal tumors: current classification and MRI features. Neuroradiology 50 (2008): 301-314.
9. Sehgal VN, Sharma S, Oberai R. Evaluation of plexiform neurofibroma in neurofibromatosis type 1 in 18 family members of 3 generations: ultrasonography and magnetic resonance imaging a diagnostic supplement Int J Dermatol 48 (2009): 275-279.

10. Kakkar C, Shetty CM, Koteshwara P, et al. Telltale signs of peripheral neurogenic tumors on magnetic resonance imaging Indian J Radiol Imaging 25 (2015): 453-458.
11. Nguyen R, Dombi E, Akshintala S, et al. Characterization of spinal findings in children and adults with neurofibromatosis type 1 enrolled in a natural history study using magnetic resonance imaging J Neurooncol 121 (2015): 209-215.
12. Feldman DS, Jordan C, Fonseca L. Orthopaedic Manifestations of Neurofibromatosis Type 1. Journal of the American Academy of Orthopaedic Surgeon 18 (2010): 346-357.
13. Patel NB, Stacy GS. Musculoskeletal Manifestations of Neurofibromatosis Type 1. AJR 199 (2012).
14. Chung JY, Kim SS, Kim SK. Spindle cell type malignant peripheral nerve sheath tumor arising in benign schwannoma with multiple intraosseous spinal metastasis: A case report. J Back Musculoskelet Rehabil 30 (2017): 1129-1135.
15. Pavlus JD, Carter BW, Tolley MD, et al. Imaging of Thoracic Neurogenic Tumors. AJR Am J Roentgenol 207 (2016): 552-561.
16. Wasa J, Nishida Y, Tsukushi S, et al. MRI features in the differentiation of malignant peripheral nerve sheath tumors and neurofibromas. AJR Am J Roentgenol 194 (2010): 1568-1574.
17. Tanaka O, Kiryu T, Hirose Y, et al. Neurogenic tumors of the mediastinum and chest wall: MR imaging appearance. J Thorac Imaging 20 (2005): 316-320.
18. Woo OH, Yong HS, Shin BK, et al. Wide spectrum of thoracic neurogenic tumours: a pictorial review of CT and pathological findings. Br J Radiol 81 (2008): 668-676.
19. Gahr N, Darge K, Hahn G, et al. Diffusion-weighted MRI for differentiation of neuroblastoma and ganglioneuroblastoma/ganglioneuroma. Eur J Radiol 79 (2011): 443-446.
20. Lee JY, Lee KS, Han J, et al. Spectrum of neurogenic tumors in the thorax: CT and pathologic findings. J Comput Assist Tomogr 23 (1999): 399-406.
21. Papaioannou G, McHugh K. Neuroblastoma in childhood: review and radiological findings. Cancer Imaging 5 (2005): 116-127
22. Houten JK, Babu RP, Miller DC. Thoracic paraganglioma presenting with spinal cord compression and metastases. J Spinal DisordTechn 15 (2002): 319-323.
23. Shin JY, Lee SM, Hwang MY, et al. MR findings of spinal paraganglioma: report of three cases. J Korean Med Sci 16 (2001): 522-526.
24. Conti P, Mouchaty, H, Spacca, B. et al. Thoracic extradural paragangliomas: a case report and review of the literature. Spinal Cord 44 (2006): 120-125.
25. Moussaly E, Nazha B, Zaarour M, et al. Primary Non-Hodgkin's Lymphoma of the Spine: A Case Report and Literature Review. World J Oncol 6 (2015): 459-463.
26. Kim DG, Nam DH, Jung HW, et al. Primary central nervous system lymphoma: variety of clinical manifestations and survival Acta Neurochir 138 (1996): 280-289.
27. Seo, JY, Ha, KY, Kim, MU. et al. Spinal cord compression by B-cell lymphoma, unclassifiable, with features intermediate between diffuse large B-cell lymphoma and Burkitt lymphoma in a patient seropositive for human immunodeficiency virus: a case report. J Med Case Reports 8 (2014): 324.

28. Harris E, Butler JS, Cassidy N. Aggressive plasmablastic lymphoma of the thoracic spine presenting as acute spinal cord compression in a case of asymptomatic undiagnosed human immunodeficiency virus infection. Spine J. 14 (2014): e1-e5.
29. Grier HE. The Ewing family of tumors. Ewing's sarcoma and primitive neuroectodermal tumors. Pediatr Clin North Am 44 (1997): 991-1004.
30. Tateishi U, Gladish GW, Kusumoto M, et al. Chest Wall Tumors: Radiologic Findings and Pathologic Correlation. Radio Graphics 23 (2003): 1491-1508.
31. Gladish GW, Sabloff BM, Munden RF, et al. Primary thoracic sarcomas. Radiographics 22 (2002): 621-637.
32. Murphey MD, Senchak LT, Mambalam PK, et al. From the radiologic pathology archives: ewing sarcoma family of tumors: radiologic-pathologic correlation. Radiographics 33 (2013): 803-831.
33. Treu EB, de Slegte RG, Golding RP, et al. CT findings in paravertebral synovial sarcoma. J Comput Assist Tomogr 10 (1986): 460-462.
34. Sang-il Suh, Hae Young Seol, Suk-Joo Hong, et al. American Spinal Epidural Synovial Sarcoma: A Case of Homogeneous Enhancing Large Paravertebral Mass on MR Imaging Journal of Neuroradiology October 26 (2005): 2402-2405.
35. Maccauro G, Spinelli MS, Mauro S, et al. Physiopathology of spine metastasis. Int J Surg Oncol (2011): 107969.
36. Gala FB, Aswani Y. Imaging in spinal posterior epidural space lesions: A pictorial essay. Indian J Radiol Imaging. 26 (2016): 299-315.
37. Mendel E, Bourekas E, Gerszten P, et al. Percutaneous techniques in the treatment of spine tumors: what are the diagnostic and therapeutic indications and outcomes? Spine (Phila Pa 1976) 34 (2009): S93-S100.
38. Haidar R, Mhaidli H, Taher AT. Paraspinal extramedullary hematopoiesis in patients with thalassemia intermedia. Eur Spine J 19 (2010): 871-878.
39. Zhu G, Wu X, Zhang X, et al. Clinical and imaging findings in thalassemia patients with extramedullary hematopoiesis. Clinical Imaging 36 (2012): 475-482.
40. Tsitouridis J, Stamos S, Hassapopoulou E, et al. Extramedullary paraspinal hematopoiesis in thalassemia: CT and MRI evaluation European Journal of Radiology 30 (1999): 33-38.
41. Dibbern D, Loevner L, Lieberman A, et al. MR of thoracic cord compression caused by epidural extramedullary hematopoiesis in myelodysplastic syndrome. Am J Roentgenol 18 (1997): 363-366.
42. Van Tassel P. Magnetic resonance imaging of spinal infections. Top MagnReson Imaging 6 (1994): 69-81.
43. Millot F, Bonnaire B, Clavel G, et al. Hematogenous Staphylococcus aureus discitis in adults can start outside the vertebral body. Joint Bone Spine 77 (2010): 76-77.
44. Caranci F, Tedeschi E, Ugga L, et al. Magnetic Resonance Imaging correlates of benign and malignantalterations of the spinal bone marrow. Acta Biomed. 89 (2018): 18-33.
45. Kumar Y, Gupta N, Chhabra A, et al. Magnetic resonance imaging of bacterial and tuberculous spondylodiscitis with associated complications and non-infectious spinal pathology mimicking infections: a pictorial review. BMC MusculoskeletDisord. 18 (2017): 244.

46. Dagirmanjian A, Schils J, McHenry MC. MR imaging of spinal infections. MagnReson Imaging Clin N Am 7 (1999): 525-538.
47. Rivas-Garcia A, Sarria-Estrada S, Torrents-Odin C, et al. Imaging findings of Pott's disease. Eur Spine J. 22 (2013): 567-578.
48. Hong SH, Choi J-Y, Lee JW, et al. MR Imaging Assessment of the Spine: Infection or an Imitation? RadioGraphics 29 (2009): 599-612.
49. Ahmadi J, Bajaj A, Destian S, et al. Spinal tuberculosis: Atypical observations at MR imaging. Radiology 189 (1993): 489-493.
50. Mavrogenis AF, Megaloikonomos PD, Igoumenou VG, et al. Spondylodiscitis revisited. EFORT Open Rev. 2 (2017): 447-461.